

## The pGinger family of expression plasmids

Allison N. Pearson<sup>1,2,3\*</sup>, Mitchell G. Thompson<sup>1,4\*</sup>, Liam D. Kirkpatrick<sup>1,4</sup>, Cindy Ho<sup>1,2</sup>, Khanh M. Vuu<sup>1,4</sup>, Lucas M. Waldburger<sup>1,2,5</sup>, Jay D. Keasling<sup>1,2,6,7,8†</sup>, Patrick M. Shih<sup>1,3,4,9†</sup>

<sup>1</sup>Joint BioEnergy Institute, 5885 Hollis Street, Emeryville, CA 94608, USA.

<sup>2</sup>Biological Systems & Engineering Division, Lawrence Berkeley National Laboratory, Berkeley, CA 94720, USA.

<sup>3</sup>Department of Plant and Microbial Biology, University of California, Berkeley, CA 94720, USA

<sup>4</sup>Environmental Genomics and Systems Biology Division, Lawrence Berkeley National Laboratory, Berkeley, California, USA

<sup>5</sup>Department of Bioengineering, University of California, Berkeley, California, USA

<sup>6</sup>Department of Chemical and Biomolecular Engineering, University of California, Berkeley, CA 94720, USA

<sup>7</sup>The Novo Nordisk Foundation Center for Biosustainability, Technical University of Denmark, Denmark

<sup>8</sup>Center for Synthetic Biochemistry, Institute for Synthetic Biology, Shenzhen Institutes for Advanced Technologies, Shenzhen, China

<sup>9</sup>Innovative Genomics Institute, University of California, Berkeley, CA

\*Allison N. Pearson and Mitchell G. Thompson contributed equally to this manuscript

†Correspondence should be addressed to either Jay D. Keasling ([jdkeasling@lbl.gov](mailto:jdkeasling@lbl.gov)) or Patrick M. Shih ([pmshih@lbl.gov](mailto:pmshih@lbl.gov))

### Abstract

The pGinger suite of expression plasmids comprises 43 plasmids that will enable precise constitutive and inducible gene expression in a wide range of gram-negative bacterial species. Constitutive vectors are composed of 16 synthetic constitutive promoters upstream of RFP, with a broad host range BBR1 origin and a kanamycin resistance marker. The family also has seven inducible promoters (Jungle Express, NahR, XylS, RhaS, Lac, LacUV5, and TetR) controlling RFP expression on BBR1/kanamycin plasmid backbones. For four of these inducible promoters (Jungle Express, NahR, Lac, and TetR), we created variants that utilize the RK2 origin and spectinomycin or gentamicin selection. Relevant RFP expression and growth data have been

35 collected in the model bacterium *Escherichia coli* as well as *Pseudomonas putida*. All pGinger  
36 vectors are available via the Joint BioEnergy Institute (JBEI) Public Registry.

## 37 **Introduction**

38       Precise and reliable control over gene expression is one of the most fundamental  
39 requirements of synthetic biology (1). Consequently, there has been considerable effort towards  
40 identifying myriad genetic elements that enable researchers to regulate the strength and timing of  
41 transcription across all domains of life (2–4). The end result of these efforts are often  
42 consolidated families of plasmid vectors that facilitate advanced genetic engineering, such as the  
43 BglBrick family of plasmids for *E. coli* (5, 6) and the jStack vectors used in multiple plant  
44 species (7). However, as the field of synthetic biology moves beyond traditional model  
45 organisms, families of expression vectors must be tailored to meet the specific requirements of  
46 particular hosts. Advances in non-model organisms often come in the form of species or genus  
47 specific toolkits (8, 9), though more recently comprehensive plasmid toolkits have been  
48 developed and validated for a wide range of gram-negative organisms (10). Still, given that many  
49 bacteria require very particular combinations of promoters, origins, and selectable markers to  
50 enable controlled gene expression, there remains a need for vectors that will allow rapid  
51 prototyping of genetic circuits in understudied bacteria.

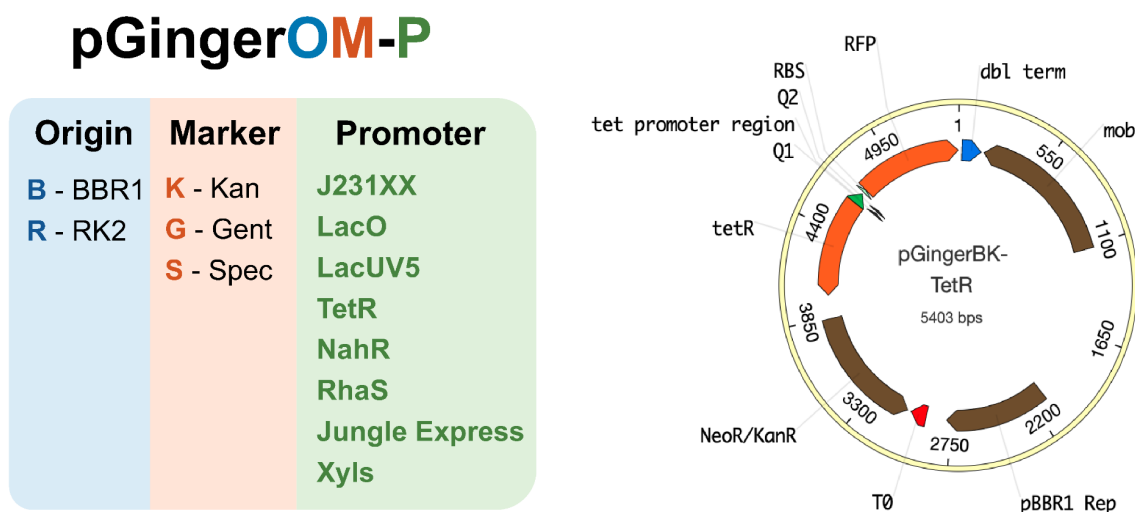
52       To facilitate the exploration of non-model hosts, we have developed a small suite of  
53 plasmids that permit both constitutive and inducible expression from the broad host-range origin  
54 of replication BBR1 using a kanamycin selection marker. For a subset of the inducible promoters  
55 that are known to work across multiple hosts, we have assembled combinatorial variants that  
56 utilize the compatible broad host-range origin RK2 (11) as well as both spectinomycin and  
57 gentamicin selection markers. This family of plasmids, which we have named the pGinger suite,

58 requires no assembly of these parts, can be easily cloned into via standard Gibson assembly  
59 techniques, and has both digital sequences and physical samples that can be publicly accessed  
60 through the Joint BioEnergy Institute (JBEI) registry (12).

## 61 Results

### 62 Design and Architecture of pGinger Plasmids

63 All pGinger vectors express RFP with a consensus ribosomal binding site (RBS -  
64 TTTAAGAAGGAGATATACAT) derived from the BglBrick plasmid library. The overall  
65 conserved plasmid architecture and naming convention of the pGinger suite are shown in **Figure**  
66 **1**.



67  
68 **Figure 1: Plasmids architecture of the pGinger suite:** The pGinger plasmids share a common naming convention  
69 where the first two letters after pGinger correspond to the origin and resistance marker respectively, followed by the  
70 promoter. All plasmids share the same architecture as the above map of pGingerBK-TetR, whereby a conserved  
71 RBS-RFP is downstream of the promoter followed by a strong terminator. All selectable markers are upstream of  
72 the promoter, with the origin between the marker and the RFP cassette.

73

74 The BBR1 origin and kanamycin cassette of relevant pGinger vectors were both derived from  
75 plasmid pBADTrfp (13). To develop a family of constitutive expression plasmids, the AraC  
76 coding sequence and promoter of pBADTrfp were replaced with 16 different synthetic promoters  
77 from the Anderson Promoter Library (<http://parts.igem.org/Promoters/Catalog/Anderson>). For  
78 the inducible vectors, the AraC coding sequence and promoter of pBADTrfp were replaced with  
79 the following seven inducible systems: Jungle Express - derived from pTR\_sJExD-rfp (14);  
80 NahR - derived from pPS43 (15); RhaS - derived from pCV203 (15); TetR - derived from  
81 pBbE2a-RFP; XylS - derived from pPS66 (15); Lac - derived from pBbE6a-RFP (6); LacUV5 -  
82 derived from pBbE5a-RFP (6). For four of the inducible promoters (Jungle Express, NahR, Lac,  
83 and TetR), additional vectors were constructed that varied both the origin and antibiotic marker.  
84 All RK2 origins were derived from pBb(RK2)1k-GFPuv (8), while the gentamicin resistance  
85 cassette was derived from pMQ30 (16), and the spectinomycin cassette was derived from  
86 pSR43.6 (17). All BBR1 derivatives of pBADTrfp contain the *mob* element that facilitates  
87 conjugal transfer. A full description of each pGinger vector can be found in **Table 1**.

88

89

Name	Origin	Marker	Promoter Class	Promoter	Inducer	JBEI ICE No.
pGingerBK-J23100	BBR1	Kanamycin	Constitutive	J23100	NA	JPUB_020797
pGingerBK-J23101	BBR1	Kanamycin	Constitutive	J23101	NA	JPUB_020799
pGingerBK-J23102	BBR1	Kanamycin	Constitutive	J23102	NA	JPUB_020815
pGingerBK-J23103	BBR1	Kanamycin	Constitutive	J23103	NA	JPUB_020801
pGingerBK-J23104	BBR1	Kanamycin	Constitutive	J23104	NA	JPUB_020803
pGingerBK-J23105	BBR1	Kanamycin	Constitutive	J23105	NA	JPUB_020817
pGingerBK-J23106	BBR1	Kanamycin	Constitutive	J23106	NA	JPUB_020793
pGingerBK-J23107	BBR1	Kanamycin	Constitutive	J23107	NA	JPUB_020819
pGingerBK-J23108	BBR1	Kanamycin	Constitutive	J23108	NA	JPUB_020821

pGingerBK-J23110	BBR1	Kanamycin	Constitutive	J23110	NA	JPUB_020805
pGingerBK-J23111	BBR1	Kanamycin	Constitutive	J23111	NA	JPUB_020807
pGingerBK-J23113	BBR1	Kanamycin	Constitutive	J23113	NA	JPUB_020809
pGingerBK-J23114	BBR1	Kanamycin	Constitutive	J13114	NA	JPUB_020811
pGingerBK-J23117	BBR1	Kanamycin	Constitutive	J13117	NA	JPUB_020795
pGingerBK-J23118	BBR1	Kanamycin	Constitutive	J23118	NA	JPUB_020823
pGingerBK-J23119	BBR1	Kanamycin	Constitutive	J23119	NA	JPUB_020813
pGingerBK-JE	BBR1	Kanamycin	Inducible	Jungle Express	Crystal Violet	JPUB_020825
pGingerBK-NahR	BBR1	Kanamycin	Inducible	NahR	Salicylic acid	JPUB_020831
pGingerBK-RhaS	BBR1	Kanamycin	Inducible	RhaS	Rhamnose	JPUB_020829
pGingerBK-TetR	BBR1	Kanamycin	Inducible	TetR	Oxytetracycline	JPUB_020835
pGingerBK-XylS	BBR1	Kanamycin	Inducible	XylS	Benzoate	JPUB_020827
pGingerBK-Lac	BBR1	Kanamycin	Inducible	Lac	IPTG	JPUB_020833
pGingerBK-LacUV5	BBR1	Kanamycin	Inducible	LacUV5	IPTG	JPUB_020837
pGingerBG-JE	BBR1	Gentamicin	Inducible	Jungle Express	Crystal Violet	JPUB_020847
pGingerBS-JE	BBR1	Spectinomycin	Inducible	Jungle Express	Crystal Violet	JPUB_020855
pGingerRK-JE	RK2	Kanamycin	Inducible	Jungle Express	Crystal Violet	JPUB_020871
pGingerRG-JE	RK2	Gentamicin	Inducible	Jungle Express	Crystal Violet	JPUB_020881
pGingerRS-JE	RK2	Spectinomycin	Inducible	Jungle Express	Crystal Violet	JPUB_020863
pGingerBG-NahR	BBR1	Gentamicin	Inducible	NahR	Salicylic acid	JPUB_020845
pGingerBS-NahR	BBR1	Spectinomycin	Inducible	NahR	Salicylic acid	JPUB_020853
pGingerRK-NahR	RK2	Kanamycin	Inducible	NahR	Salicylic acid	JPUB_020869
pGingerRG-NahR	RK2	Gentamicin	Inducible	NahR	Salicylic acid	JPUB_020879
pGingerRS-NahR	RK2	Spectinomycin	Inducible	NahR	Salicylic acid	JPUB_020859
pGingerBG-TetR	BBR1	Gentamicin	Inducible	TetR	Oxytetracycline	JPUB_020843
pGingerBS-TetR	BBR1	Spectinomycin	Inducible	TetR	Oxytetracycline	JPUB_020851
pGingerRK-TetR	RK2	Kanamycin	Inducible	TetR	Oxytetracycline	JPUB_020865
pGingerRG-TetR	RK2	Gentamicin	Inducible	TetR	Oxytetracycline	JPUB_020877
pGingerRS-TetR	RK2	Spectinomycin	Inducible	TetR	Oxytetracycline	JPUB_020861
pGingerBG-Lac	BBR1	Gentamicin	Inducible	Lac	IPTG	JPUB_020841
pGingerBS-Lac	BBR1	Spectinomycin	Inducible	Lac	IPTG	JPUB_020849

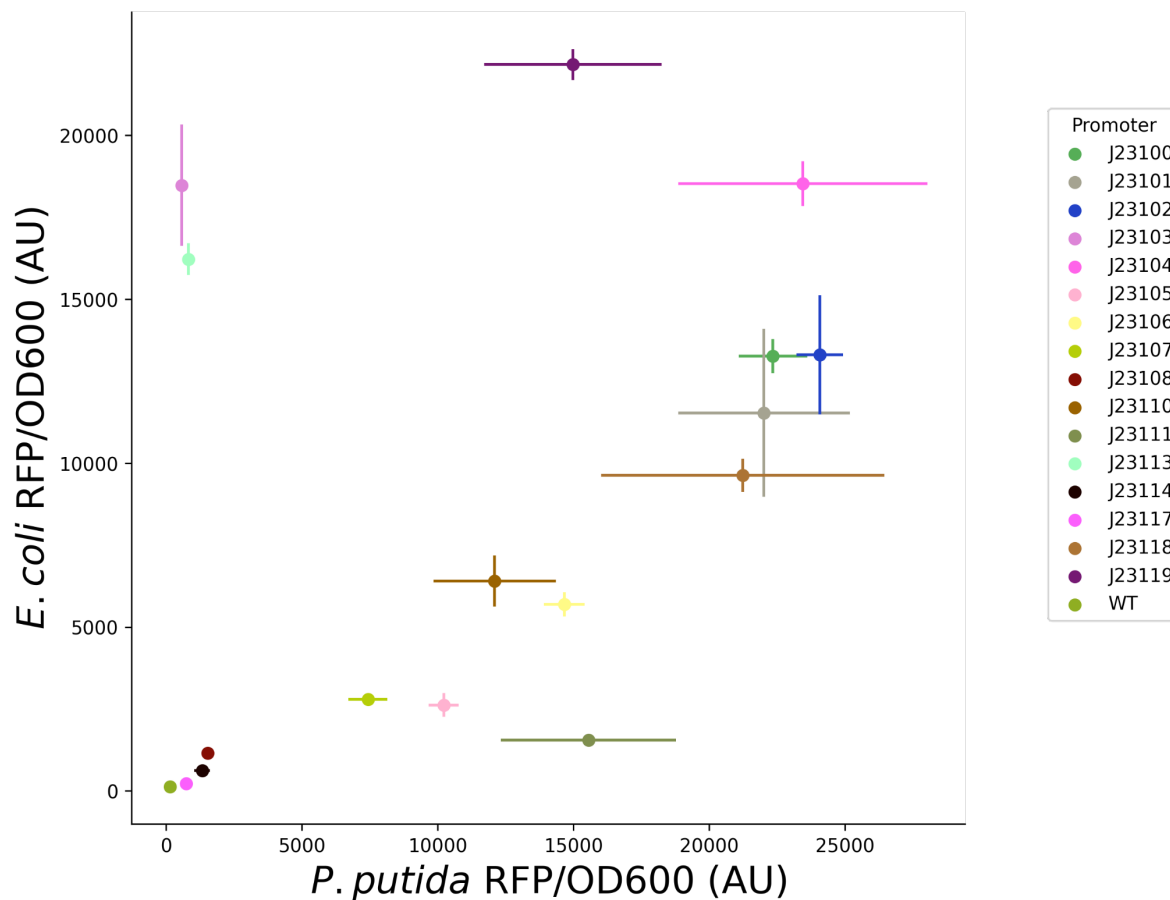
pGingerRK-Lac	RK2	Kanamycin	Inducible	Lac	IPTG	JPUB_020867
pGingerRG-Lac	RK2	Gentamicin	Inducible	Lac	IPTG	JPUB_020875
pGingerRS-Lac	RK2	Spectinomycin	Inducible	Lac	IPTG	JPUB_020857

90

91 **Table 1: Plasmids in the pGinger suite:** Relevant characteristics of pGinger plasmids including origin of  
92 replication, antibiotic selection, promoter characteristics, and if applicable inducing molecule. JBEI public registry  
93 numbers are also included for digital accessibility.

#### 94 Evaluation of Constitutive Expression pGinger Plasmids

95 To evaluate the relative strength of constitutive Anderson promoters in the context of the  
96 pGinger vectors, plasmids were introduced into both *P. putida* and *E. coli*. Fluorescence was  
97 measured after growth in LB medium after 24 hours. When fluorescence was normalized to cell  
98 density, expression from Anderson promoters showed significant correlation (Spearman's  $\rho =$   
99  $0.49$ ,  $p = 0.045$ ) between *P. putida* and *E. coli* (**Figure 2**). Promoters J23103 and J23113 were  
100 significantly stronger in *E. coli* than in *P. putida*, while promoter J23111 was significantly  
101 stronger in *P. putida*. Promoter sequences and mean expression values in both *E. coli* and *P.*  
102 *putida* are listed in **Table 2**.



103

104 **Figure 2: Activity of Constitutive Promoters in *E. coli* and *P. putida*.** RFP expression normalized to cell density

105 from Anderson promoters within either *E. coli* (y-axis) or *P. putida* (x-axis) are shown with standard deviations (

106 n=3).

107

Promoter	Promoter Sequence	<i>E. coli</i> expression	<i>P. putida</i> expression
J23100	ttgacggctagctcagtcctaggtacagtgctagc	13267 (+/- 517)	22343 (+/- 1262)
J23101	tttacagctagctcagtcctaggtattatgctagc	11530 (+/- 2565)	22010 (+/- 3162)
J23102	ttgacagctagctcagtcctaggtactgtgctagc	13300 (+/- 1815)	24067 (+/- 858)
J23103	ctgatagctagctcagtcctagggattatgctagc	18476 (+/- 1857)	565 (+/- 135)
J23104	ttgacagctagctcagtcctaggtattgtgctagc	18522 (+/- 682)	23440 (+/- 4588)
J23105	tttacggctagctcagtcctaggtactatgctagc	2622 (+/- 363)	10220 (+/- 558)

J23106	tttacggctagctcagtcctaggtatagtgtctagc	5697 (+/- 369)	14659 (+/- 748)
J23107	tttacggctagctcagccctaggtattatgtctagc	2798 (+/- 44)	7429 (+/- 716)
J23108	ctgacagctagctcagtcctaggtataatgtctagc	1149 (+/- 84)	1523 (+/- 84)
J23110	tttacggctagctcagtcctaggtacaatgtctagc	6402 (+/- 782)	12098 (+/- 2251)
J23111	ttgacggctagctcagtcctaggtatagtgtctagc	1547 (+/- 106)	15548 (+/- 3229)
J23113	ctgatggctagctcagtcctagggattatgtctagc	16220 (+/- 480)	826 (+/- 92)
J23114	tttatggctagctcagtcctaggtacaatgtctagc	625 (+/- 48)	1325 (+/- 289)
J23117	ttgacagctagctcagtcctagggattgtgtctagc	229 (+/- 25)	730 (+/- 28)
J23118	ttgacggctagctcagtcctaggtattgtgtctagc	9628 (+/- 507)	21237 (+/- 5215)
J23119	ttgacagctagctcagtcctaggtataatgtctagc	22157 (+/- 473)	14979 (+/- 3262)
WT	NA	124 (+/- 6)	141 (+/- 17)

108

109 **Table 2: Expression of pGinger Anderson promoters:** For each Anderson promoter the sequence is provided as  
 110 well as the mean cell density normalized RFP fluorescence in both *E. coli* and *P. putida*. Standard deviations are  
 111 provided in parentheses, n=3.

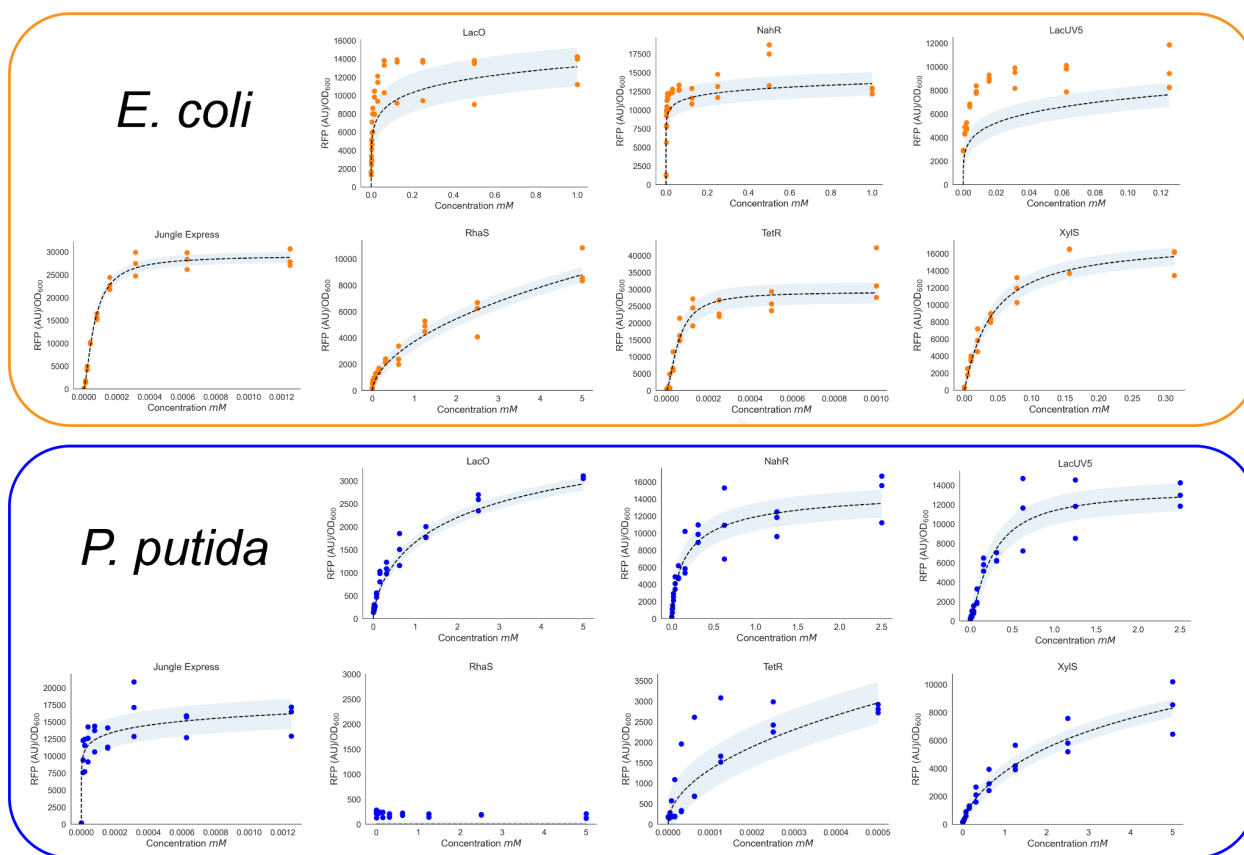
112

### 113 Evaluation of Inducible pGinger Plasmids

114 The expression of the seven inducible promoters within the pGinger suite was evaluated  
 115 using the BBR1 origin and kanamycin marker (pGingerBK) against a titration of the inducer in  
 116 both *E. coli* and *P. putida* (**Figure 3**). All promoters showed inducibility in *E. coli*, and all but  
 117 the rhamnose inducible RhaS promoter showed inducibility in *P. putida*. Relevant expression  
 118 characteristics of the inducible pGingerBK vectors in both tested bacteria are listed in **Table 3**.  
 119 The strongest normalized expression from an inducible promoter in *E. coli* was the TetR system,  
 120 while both the strongest promoters in *P. putida* were found to be NahR and Jungle Express



121 promoters, which showed nearly identical maximal expression. In both bacteria, the Jungle  
 122 Express promoter demonstrated the greatest level of induction relative to background expression.



123  
 124 **Figure 3: Activity of Inducible Promoters in *E. coli* and *P. putida*.** RFP expression normalized to cell density (y-  
 125 axis) from inducible promoters within either *E. coli* (top panel in orange) or *P. putida* (bottom panel in blue) as a  
 126 function of inducer concentration in mM (x-axis). Fits to the Hill equation are shown as dashed lines and shaded to  
 127 show confidence intervals. Raw data points are overlaid (n=3).

128

Promoter	Organism	Background	Max Exp.	Max Conc.	Induction
LacO	<i>E. coli</i>	1510 (+/- 186)	13127 (+/- 1693)	1 mM	9x
	<i>P. putida</i>	137 (+/- 5)	3074 (+/- 30)	5 mM	22x
NahR	<i>E. coli</i>	1260 (+/- 57)	16484 (+/- 1693)	500 uM	9x
	<i>P. putida</i>	847 (+/- 244)	25697 (+/- 2976)	5 mM	30x

LacUV5	<i>E. coli</i>	2889 (+/- 36)	10137 (+/- 855)	250 uM	4x
	<i>P. putida</i>	203 (+/- 53)	16622 (+/- 3671)	10 mM	82x
Jungle Express	<i>E. coli</i>	100 (+/- 2)	28545 (+/- 1890)	125 nM	285x
	<i>P. putida</i>	183 (+/- 1)	16956 (+/- 4002)	313 nM	93x
RhaS	<i>E. coli</i>	172 (+/- 42)	9251 (+/- 1389)	5 mM	54x
	<i>P. putida</i>	NA	NA	NA	NA
TetR	<i>E. coli</i>	341 (+/- 10)	33631 (+/- 7692)	1 uM	98x
	<i>P. putida</i>	176 (+/- 9)	3214 (+/- 319)	1 uM	18x
XylS	<i>E. coli</i>	329 (+/- 57)	15280 (+/- 1590)	313 uM	46x
	<i>P. putida</i>	161 (+/- 7)	8401 (+/- 1877)	5 mM	52x

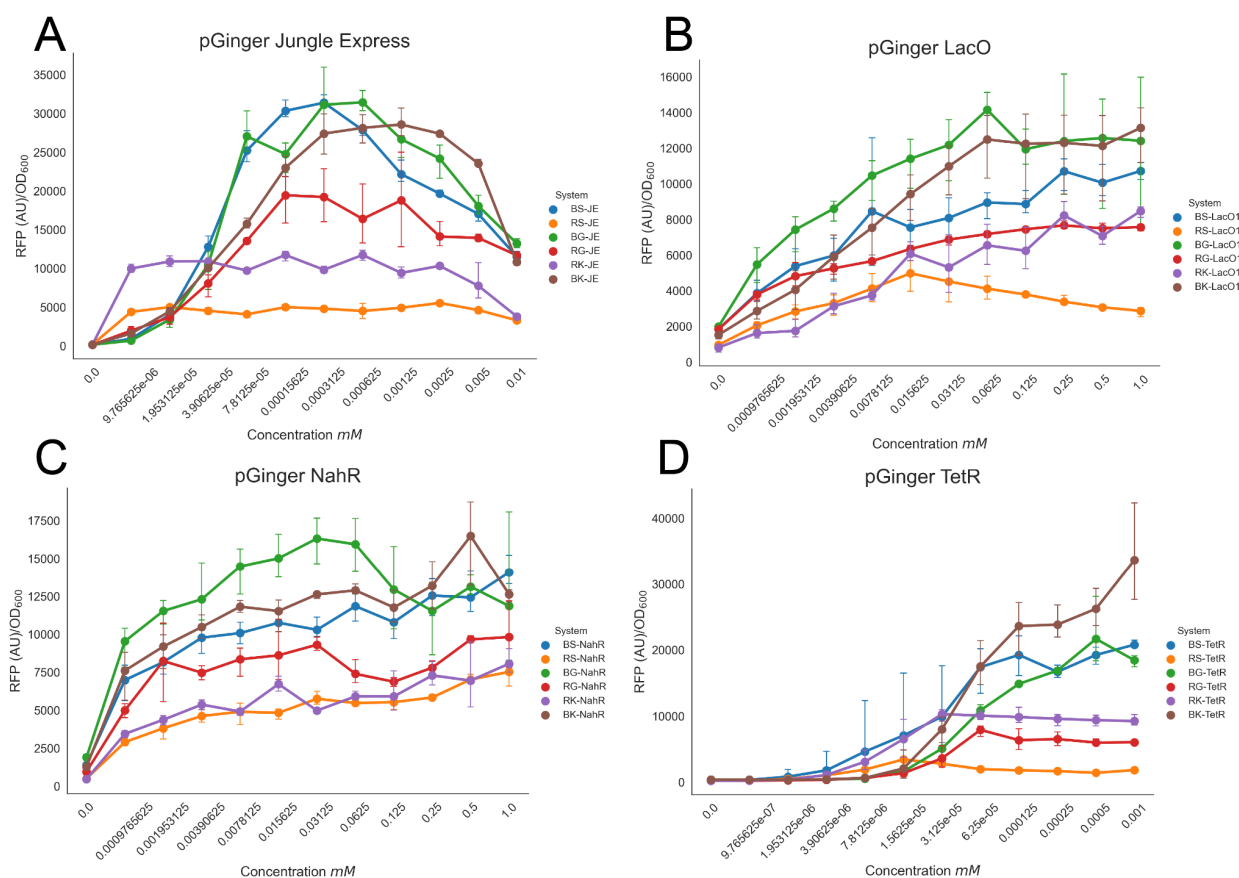
129

130 **Table 3: Inducible Promoters in *E. coli* and *P. putida*:** For each inducible promoter on a BBR1 origin with a  
 131 kanamycin marker, the experimentally observed background (uninduced) fluorescence and maximal fluorescence  
 132 are given for both *E. coli* and *P. putida*. Standard deviations are provided in parentheses, n=3. Additionally, the  
 133 inducer concentration used to achieve maximal expression and the relative induction levels are listed.

134

135 To evaluate the effect of varying origin and selectable markers on expression from  
 136 inducible promoters, all six variants of the Jungle Express, LacO, NahR, and TetR were  
 137 investigated for their dose-response to their inducer molecules in *E. coli* (**Figure 4**). Relevant  
 138 expression parameters are listed in **Table 4**. In general, BBR1 variants showed greater  
 139 expression than RK2 origin plasmids, which is expected given the higher copy of BBR1  
 140 plasmids in *E. coli* (10). Amongst the pGinger Jungle Express vectors, both pGingerRS-JE and  
 141 pGingerRK-JE showed dose-responses distinct from the other vectors (**Figure 4A**). Notably, all

142 pGingerRS (RK2-Spectinomycin) plasmids showed the lowest expression across each promoter  
 143 tested (Table 4).



144  
 145 **Figure 4: Activity of Inducible pGinger variants in *E. coli*.** For origin and selection marker pGinger variants of  
 146 Jungle Express (A), LacO (B), NahR (C), and TetR (D), dose-response curves of normalized RFP expression are  
 147 shown as a function of mM inducer. Error bars represent standard deviations (n=3). Note that the x-axis is non-  
 148 linear.

149

Promoter	Origin	Marker	Background	Max Exp.	Max Conc.	Induction
LacO	BBR1	Kan	1510 (+/- 186)	13127 (+/- 1693)	1 mM	9x
LacO	BBR1	Gent	1976 (+/- 70)	14143 (+/- 1608)	63 uM	7x
LacO	BBR1	Spec	1830 (+/- 320)	10694 (+/- 943)	250 uM	6x

LacO	RK2	Kan	803 (+/- 216)	8213 (+/- 721)	250 uM	10x
LacO	RK2	Gent	1823 (+/- 78)	7654 (+/- 230)	250 uM	4x
LacO	RK2	Spec	950 (+/- 46)	4967 (+/- 895)	16 uM	5x
NahR	BBR1	Kan	1260 (+/- 57)	16484 (+/- 1693)	500 uM	9x
NahR	BBR1	Gent	1877 (+/- 334)	16317 (+/- 1534)	31 uM	9x
NahR	BBR1	Spec	1372 (+/- 84)	14083 (+/- 984)	1 mM	10x
NahR	RK2	Kan	445 (+/- 39)	8048 (+/- 859)	1 mM	18x
NahR	RK2	Gent	934 (+/- 56)	9299 (+/- 460)	1 mM	10x
NahR	RK2	Spec	482 (+/- 69)	7510 (+/- 817)	1 mM	16x
Jungle Express	BBR1	Kan	100 (+/- 2)	28545 (+/- 1890)	125 nM	285x
Jungle Express	BBR1	Gent	124 (+/- 24)	31409 (+/- 1348)	625 nM	254x
Jungle Express	BBR1	Spec	107 (+/- 9)	31360 (+/- 905)	313 nM	292x
Jungle Express	RK2	Kan	151 (+/- 25)	11702 (+/- 3180)	625 nM	78x
Jungle Express	RK2	Gent	91 (+/- 6)	19413 (+/- 3180)	156 nM	214x
Jungle Express	RK2	Spec	153 (+/- 18)	4978 (+/- 305)	20 nM	32x
TetR	BBR1	Kan	341 (+/- 10)	33631 (+/- 7692)	1 uM	98x
TetR	BBR1	Gent	351 (+/- 32)	21646 (+/- 5579)	500 nM	62x
TetR	BBR1	Spec	232 (+/- 43)	19224 (+/- 3027)	125 nM	83x
TetR	RK2	Kan	184 (+/- 5)	10281 (+/- 967)	31 nM	56x
TetR	RK2	Gent	232 (+/- 39)	7883 (+/- 865)	63 nM	34x
TetR	RK2	Spec	197 (+/- 5)	3399 (+/- 143)	16 nM	17x

150

151 **Table 4: Inducible pGinger variants in *E. coli*:** For pGinger variants of LacO, NahR, Jungle Express, and TetR

152 promoters, the experimentally observed background (uninduced) fluorescence and maximal fluorescence in *E. coli*

153 are provided. Standard deviations are provided in parentheses, n=3. Additionally, the inducer concentration used to  
154 achieve maximal expression and the relative induction levels are listed.

155

156

## 157 **Discussion**

158 The pGinger suite of plasmids offers researchers an array of small, pre-assembled vectors  
159 that will permit rapid identification of useful genetic elements in diverse gram-negative bacteria  
160 due to the use of broad host-range origins (RK2) and selectable markers known to work across  
161 many species (kanamycin, spectinomycin, gentamicin). The compatibility of RK2 and BBR1  
162 origins may also permit researchers to introduce multiple pGinger vectors into a single strain  
163 simultaneously (11). In combination with other recent plasmid suites that have been publicly  
164 released, the pGinger plasmids have the potential to facilitate more advanced synthetic biology  
165 and metabolic engineering efforts in bacterial species that have been traditionally understudied.

## 166 **Materials & Methods**

### 167 Strains and Media

168 Cultures were grown in lysogeny broth (LB) Miller medium (BD Biosciences, USA) at  
169 37 °C for *E. coli* XL1-Blue (QB3 Macrolab, USA) and 30 °C for *P. putida* KT2440 (ATCC  
170 47054). The medium was supplemented with kanamycin (50 mg/L, Sigma Aldrich, USA),  
171 gentamicin (30 mg/L, Fisher Scientific, USA), or spectinomycin (100mg/L, Sigma Aldrich,  
172 USA), when indicated. All other compounds were purchased through Sigma Aldrich (Sigma  
173 Aldrich, USA).

### 174 Plasmid Design and Construction

175 All plasmids were designed using Device Editor and Vector Editor software, while all  
176 primers used for the construction of plasmids were designed using j5 software (12, 18, 19).  
177 Plasmids were assembled via Gibson Assembly using standard protocols (20). Plasmids were  
178 routinely isolated using the Qiaprep Spin Miniprep kit (Qiagen, USA), and all primers were  
179 purchased from Integrated DNA Technologies (IDT, Coralville, IA).

#### 180 Plasmid and Sequence Availability

181 All strains and plasmids from Table 1 can be found via the following link to the JBEI  
182 Public Registry: <https://public-registry.jbei.org/folders/771>.

#### 183 Characterization assays

184 To characterize RFP expression from these vectors, we measured optical density and  
185 fluorescence after growth in 96 well plates for 24 hours. First, overnight cultures were inoculated  
186 into 5 mL of LB medium from single colonies and grown at 30 °C or 37 °C. These cultures were  
187 then diluted 1:100 into 500 µL of LB medium with the appropriate antibiotic in 96 square v-  
188 bottom deep well plates (Biotix™ DP22009CVS). For characterization of the inducible systems,  
189 inducer was added to wells in the first column of the plate at the maximum concentration tested  
190 and diluted two-fold across the plate until the last column, which was left as the zero-inducer  
191 control. Plates were sealed with a gas-permeable microplate adhesive film (Axygen™ BF400S)  
192 and grown for 24 hours at either 30 °C or 37 °C with shaking at 200 rpm. Optical density was  
193 measured at 600 nm, and fluorescence was measured at an excitation wavelength of 535 nm and  
194 an emission wavelength of 620 nm. All data was analyzed and visualized using custom Python  
195 scripts using the SciPy (22), NumPy (23), Pandas, Matplotlib, and Seaborn libraries. Fits to the  
196 Hill equation were done as previously described (24).

## 197 **Acknowledgements**

198           The order of authors was determined by who has the reddest hair. Mitchell Thompson is a  
199 Simons Foundation Awardee of the Life Sciences Research Foundation. Lucas Waldburger is  
200 funded by the National Science Foundation Graduate Research Fellowship. This work was part  
201 of the DOE Joint BioEnergy Institute (<https://www.jbei.org>) supported by the U.S. Department  
202 of Energy, Office of Science, Office of Biological and Environmental Research, supported by the  
203 U.S. Department of Energy, Energy Efficiency and Renewable Energy, Bioenergy Technologies  
204 Office, through contract DE-AC02-05CH11231 between Lawrence Berkeley National  
205 Laboratory and the U.S. Department of Energy. The views and opinions of the authors expressed  
206 herein do not necessarily state or reflect those of the United States Government or any agency  
207 thereof. Neither the United States Government nor any agency thereof, nor any of their  
208 employees, makes any warranty, expressed or implied, or assumes any legal liability or  
209 responsibility for the accuracy, completeness, or usefulness of any information, apparatus,  
210 product, or process disclosed, or represents that its use would not infringe privately owned rights.  
211 The United States Government retains and the publisher, by accepting the article for publication,  
212 acknowledges that the United States Government retains a nonexclusive, paid-up, irrevocable,  
213 worldwide license to publish or reproduce the published form of this manuscript, or allow others  
214 to do so, for United States Government purposes. The Department of Energy will provide public  
215 access to these results of federally sponsored research in accordance with the DOE Public Access  
216 Plan (<http://energy.gov/downloads/doe-public-access-plan>).

## 217 **Contributions**

218 Conceptualization; A.N.P., M.G.T.; Methodology; A.N.P., M.G.T.; Investigation, A.N.P.,  
219 M.G.T., L.D.K., K.M.V., L.M.W.; Writing – Original Draft, A.N.P., M.G.T.; Writing – Review  
220 and Editing, All authors.; Resources and supervision; P.M.S, J.D.K.

## 221 **Competing Interests**

222 J.D.K. has financial interests in Amyris, Ansa Biotechnologies, Apertor Pharma, Berkeley Yeast,  
223 Demetrix, Lygos, Napigen, ResVita Bio, and Zero Acre Farms.

## 224 **References**

- 225 1. Khalil AS, Collins JJ. 2010. Synthetic biology: applications come of age. *Nat Rev Genet*  
226 11:367–379.
- 227 2. Nielsen AAK, Segall-Shapiro TH, Voigt CA. 2013. Advances in genetic circuit design:  
228 novel biochemistries, deep part mining, and precision gene expression. *Curr Opin Chem*  
229 *Biol* 17:878–892.
- 230 3. Zhang Y, Ding W, Wang Z, Zhao H, Shi S. 2021. Development of Host-Orthogonal  
231 Genetic Systems for Synthetic Biology. *Advanced Biology* 5:e2000252.
- 232 4. Johns NI, Gomes ALC, Yim SS, Yang A, Blazejewski T, Smillie CS, Smith MB, Alm EJ,  
233 Kosuri S, Wang HH. 2018. Metagenomic mining of regulatory elements enables  
234 programmable species-selective gene expression. *Nat Methods* 15:323–329.
- 235 5. Anderson JC, Dueber JE, Leguia M, Wu GC, Goler JA, Arkin AP, Keasling JD. 2010.  
236 BglBricks: A flexible standard for biological part assembly. *J Biol Eng* 4:1.



- 237 6. Lee TS, Krupa RA, Zhang F, Hajimorad M, Holtz WJ, Prasad N, Lee SK, Keasling JD.  
238 2011. BglBrick vectors and datasheets: A synthetic biology platform for gene expression.  
239 J Biol Eng 5:12.
- 240 7. Shih PM, Vuu K, Mansoori N, Ayad L, Louie KB, Bowen BP, Northen TR, Loqué D.  
241 2016. A robust gene-stacking method utilizing yeast assembly for plant synthetic biology.  
242 Nat Commun 7:13215.
- 243 8. Cook TB, Rand JM, Nurani W, Courtney DK, Liu SA, Pfleger BF. 2018. Genetic tools for  
244 reliable gene expression and recombineering in *Pseudomonas putida*. J Ind Microbiol  
245 Biotechnol 45:517–527.
- 246 9. Phelan RM, Sachs D, Petkiewicz SJ, Barajas JF, Blake-Hedges JM, Thompson MG,  
247 Reider Apel A, Rasor BJ, Katz L, Keasling JD. 2017. Development of Next Generation  
248 Synthetic Biology Tools for Use in *Streptomyces venezuelae*. ACS Synth Biol 6:159–166.
- 249 10. Schuster LA, Reisch CR. 2021. A plasmid toolbox for controlled gene expression across  
250 the Proteobacteria. Nucleic Acids Res 49:7189–7202.
- 251 11. Pasin F, Bedoya LC, Bernabé-Orts JM, Gallo A, Simón-Mateo C, Orzaez D, García JA.  
252 2017. Multiple T-DNA Delivery to Plants Using Novel Mini Binary Vectors with  
253 Compatible Replication Origins. ACS Synth Biol 6:1962–1968.
- 254 12. Ham TS, Dmytriv Z, Plahar H, Chen J, Hillson NJ, Keasling JD. 2012. Design,  
255 implementation and practice of JBEI-ICE: an open source biological part registry platform  
256 and tools. Nucleic Acids Res 40:e141.
- 257 13. Bi C, Su P, Müller J, Yeh Y-C, Chhabra SR, Beller HR, Singer SW, Hillson NJ. 2013.  
258 Development of a broad-host synthetic biology toolbox for *Ralstonia eutropha* and its

- 259 application to engineering hydrocarbon biofuel production. *Microb Cell Fact* 12:107.
- 260 14. Ruegg TL, Pereira JH, Chen JC, DeGiovanni A, Novichkov P, Mutalik VK, Tomaleri GP,  
261 Singer SW, Hillson NJ, Simmons BA, Adams PD, Thelen MP. 2018. Jungle Express is a  
262 versatile repressor system for tight transcriptional control. *Nat Commun* 9:3617.
- 263 15. Calero P, Jensen SI, Nielsen AT. 2016. Broad-Host-Range ProUSER Vectors Enable Fast  
264 Characterization of Inducible Promoters and Optimization of p-Coumaric Acid Production  
265 in *Pseudomonas putida* KT2440. *ACS Synth Biol* 5:741–753.
- 266 16. Shanks RMQ, Kadouri DE, MacEachran DP, O’Toole GA. 2009. New yeast  
267 recombineering tools for bacteria. *Plasmid* 62:88–97.
- 268 17. Schmidl SR, Sheth RU, Wu A, Tabor JJ. 2014. Refactoring and optimization of light-  
269 switchable *Escherichia coli* two-component systems. *ACS Synth Biol* 3:820–831.
- 270 18. Chen J, Densmore D, Ham TS, Keasling JD, Hillson NJ. 2012. DeviceEditor visual  
271 biological CAD canvas. *J Biol Eng* 6:1.
- 272 19. Hillson NJ, Rosengarten RD, Keasling JD. 2012. j5 DNA assembly design automation  
273 software. *ACS Synth Biol* 1:14–21.
- 274 20. Gibson DG, Young L, Chuang R-Y, Venter JC, Hutchison CA, Smith HO. 2009.  
275 Enzymatic assembly of DNA molecules up to several hundred kilobases. *Nat Methods*  
276 6:343–345.
- 277 21. Thompson MG, Pearson AN, Barajas JF, Cruz-Morales P, Sedaghatian N, Costello Z,  
278 Garber ME, Incha MR, Valencia LE, Baidoo EEK, Martin HG, Mukhopadhyay A,  
279 Keasling JD. 2020. Identification, Characterization, and Application of a Highly Sensitive  
280 Lactam Biosensor from *Pseudomonas putida*. *ACS Synth Biol* 9:53–62.

- 281 22. Virtanen P, Gommers R, Oliphant TE, Haberland M, Reddy T, Cournapeau D, Burovski  
282 E, Peterson P, Weckesser W, Bright J, van der Walt SJ, Brett M, Wilson J, Millman KJ,  
283 Mayorov N, Nelson ARJ, Jones E, Kern R, Larson E, Carey CJ, SciPy 1.0 Contributors.  
284 2020. SciPy 1.0: fundamental algorithms for scientific computing in Python. Nat Methods  
285 17:261–272.
- 286 23. van der Walt S, Colbert SC, Varoquaux G. 2011. The NumPy Array: A Structure for  
287 Efficient Numerical Computation. Comput Sci Eng 13:22–30.
- 288 24. Thompson MG, Costello Z, Hummel NFC, Cruz-Morales P, Blake-Hedges JM, Krishna  
289 RN, Skyrud W, Pearson AN, Incha MR, Shih PM, Garcia-Martin H, Keasling JD. 2019.  
290 Robust Characterization of Two Distinct Glutarate Sensing Transcription Factors of  
291 *Pseudomonas putida* l -Lysine Metabolism. ACS Synth Biol 8:2385–2396.